Atmospheric Environment 222 (2020) 117138

Contents lists available at ScienceDirect

Atmospheric Environment

journal homepage: http://www.elsevier.com/locate/atmosenv

On the concentration differences between $PM_{2.5}$ FEM monitors and FRM samplers

Thi-Cuc Le [a], Krishna Kumar Shukla [a], Yu-Ting Chen [a], Shun-Chin Chang [b], Tsai-Yin Lin [c], Ziyi Li [d], David Y.H. Pui [e,f], Chuen-Jinn Tsai [a,*]

[a] Institute of Environmental Engineering, National Chiao Tung University, Hsinchu, Taiwan
[b] Department of Environmental Monitoring and Information Management, Environmental Protection Administration Executive Yuan, Taiwan
[c] Industrial Technology Research Institute, Hsinchu, Taiwan
[d] School of Energy and Environmental Engineering, University of Science and Technology Beijing, Beijing, China
[e] Mechanical Engineering Department, University of Minnesota, Minneapolis, USA
[f] School of Science and Engineering, The Chinese University of Hong Kong, Shenzhen, China

HIGHLIGHTS

- The FRM under-measures $PM_{2.5}$ due to evaporation loss while the TEOM-FDMS provides "actual" $PM_{2.5}$ value.
- The BAM-1020 over-measures or under-measures $PM_{2.5}$ due to aerosol water content and evaporation loss, respectively.
- Differences between the FEM and FRM values vary with the $PM_{2.5}$ concentrations, temperature, and relative humidity.
- The empirical equations can be used to convert the FEM data to FRM data or the FRM data to "actual" $PM_{2.5}$ value.

GRAPHICAL ABSTRACT

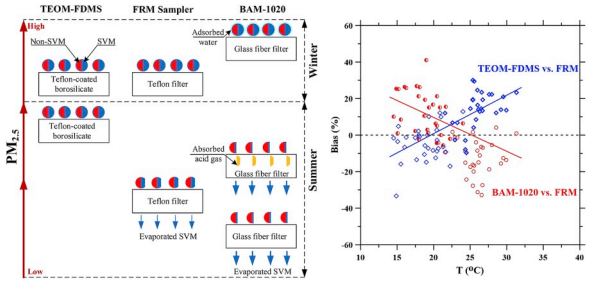

ARTICLE INFO

Keywords:
FRM samplers
FEM monitors
BAM-1020
TEOM-FDMS
$PM_{2.5}$ artifacts
Evaporation loss

ABSTRACT

BAM-1020 and TEOM-FDMS have undergone rigorous testing and analysis protocols to become the Federal Equivalent Method (FEM) monitors and serve as reliable near real-time monitors for compliance with the National Ambient Air Quality Standards and references for low-cost $PM_{2.5}$ sensor calibration. However, differences between the FEM and FRM (Federal Reference Method) data still exist, which cause inconsistency in $PM_{2.5}$ measurements. This study carried out the field tests across five geographically diverse stations in different seasons in Taiwan with 265 daily samples collected by the collocated BAM-1020 and TEOM-FDMS and the FRM sampler and found that the biases between the FEM and FRM values increased with the decreasing $PM_{2.5}$ concentrations and varied with ambient conditions. The measurement uncertainties exist in the BAM-1020 were mainly due to the aerosol water content, while the TEOM-FDMS always over-measured $PM_{2.5}$ compared to the FRM sampler since it corrects for the evaporation loss of semi-volatile particle materials. To reduce the biases between the FEM monitors and FRM samplers, empirical equations based on $PM_{2.5}$ concentrations ($\mu g\ m^{-3}$), temperature (^{o}C), and relative humidity (%) were derived to convert the FEM data to the FRM data. After correction, the mean normalized biases were decreased from $+1.67 \pm 12.43\%$ to $+0.63 \pm 8.75\%$ for the BAM-1020 and from $+13.86 \pm 14.50\%$ to $-0.85 \pm 9.0\%$ for the TEOM-FDMS. Also, the same empirical equation was

* Corresponding author.
E-mail address: cjtsai@nctu.edu.tw (C.-J. Tsai).

https://doi.org/10.1016/j.atmosenv.2019.117138
Received 4 June 2019; Received in revised form 5 November 2019; Accepted 9 November 2019
Available online 17 November 2019

used to convert the FRM $PM_{2.5}$ values to the "true" or "actual" $PM_{2.5}$ values represented by the TEOM-FDMS with the bias reduced from $-10.76 \pm 11.42\%$ to $+1.33 \pm 8.44\%$ after conversion.

1. Introduction

The accuracy of $PM_{2.5}$ (particulate matter smaller than 2.5 μm in aerodynamic diameter) measurements is important since $PM_{2.5}$ can affect human health in numerous ways (Mauderly et al., 2009; Steinle et al., 2013). Thus, the U.S. Environmental Protection Agency (EPA) enacted the Code of Federal Regulations with comprehensive specifications and explicit procedures for $PM_{2.5}$ FRM manual samplers or FEM automatic monitors to determine the compliance with the National Ambient Air Quality Standards (NAAQS) (Noble et al., 2001; U.S.EPA, 2017a). Both FRM and FEM are the standard methods for $PM_{2.5}$ measurements and can be used interchangeably for state and local air monitoring stations (SLAMS) purposes (U.S. EPA, 2016). While the FRM samplers determine 24-hr average $PM_{2.5}$ concentrations by gravimetric analysis, the FEM monitors provide 1-hr average $PM_{2.5}$ concentrations based on different principles or operation conditions (Noble et al., 2001). The FRM samplers and FEM monitors consist of a louvered PM_{10} inlet (Tolocka et al., 2001; Le et al., 2019) followed by a $PM_{2.5}$ inlet such as well impactor ninety-six (WINS, Peter et al., 2001; Le and Tsai, 2017) or very sharp cut cyclone (VSCC, Kenny et al., 2017) and a filter media to collect $PM_{2.5}$ for further analysis or direct detection.

The FEM monitors are used not only for compliance with the NAAQS but also for calibrating low-cost $PM_{2.5}$ sensors whose readings are affected by the relative humidity (RH) and $PM_{2.5}$ concentrations (Bai et al., 2019; Kuula et al., 2019; Ly et al., 2018; Johnson et al., 2018a, 2018b). However, the relevance of the FEM data to the FRM data still needs to be evaluated further since previous studies showed that FRM sampler's accuracy is affected during sampling and conditioning due to positive and negative artifacts which lead to over-measurement and under-measurement of $PM_{2.5}$ concentrations, respectively (Malm et al., 2011; Liu et al., 2014, 2015; Watson et al., 2017). The positive artifact is due to the absorption of organic/inorganic gases and water vapor by particles (Liu et al., 2014, 2015; Watson et al., 2017). Water absorption by particles exhibits a hysteretic behavior that particles start to absorb water when the RH is higher than the deliquescence RH (DRH), and water still retains on particles until the RH is lower than the efflorescence RH (ERH) when crystallization finally occurs (Seinfeld and Pandis, 2006; Watson et al., 2017). The DRH and ERH of most of the particles vary from 40 to 80% and 35–60%, respectively, depending on particle compositions (Seinfeld and Pandis, 2006). Water will evaporate from particles collected on the filter media due to the increased pressure drop across the filter during sampling resulting in the reduction of water content in particles (Chang and Tsai, 2003). However, residual water can account for as much as 20–35% $PM_{2.5}$ mass depending on $PM_{2.5}$ mass, the fraction of soluble components, and acidity of particles at the conditioning temperature (T) of 20 °C and RH of 50% required by European Committee for Standardization (Tsyrol, 2005). The composition of particles is affected significantly by the amount of water since it can change the partitioning of semi-volatile species between the gas and particle phases (Khlystov et al., 2005). The effect of aerosol water content on the FRM $PM_{2.5}$ concentrations may be ignored since the FRM $PM_{2.5}$ concentrations are determined after 24-hr conditioning at the T of 20–23 °C with a variability of $<\pm 2$ °C and the RH of 30–40% with a variability of $<\pm 5\%$ (Zhu et al., 2007; U.S. EPA, 2016).

On the other hand, the negative artifact due to the volatilization loss of semi-volatile material (SVM) causes the FRM $PM_{2.5}$ concentrations to deviate from the accurate values (Cheng and Tsai, 1997; Malm et al., 2011; Liu et al., 2014, 2015). The evaporation loss in $PM_{2.5}$ could account for as much as 5.8–36.0% "true" or "actual" $PM_{2.5}$ concentrations (Liu et al., 2014). The $PM_{2.5}$ evaporation loss in the FRM was shown to be affected by $PM_{2.5}$ concentrations, ambient temperature, relative humidity, gas-to-particle ratio (Liu et al., 2015), and the pressure drop across the filter (Grover et al., 2008). The volatilization loss also occurs during filter storage and conditioning, although it is less than that during sampling (Liu et al., 2014). The positive and negative artifacts can be corrected by using denuder samplers assembled with backup filters (Liu et al., 2011). The denuder samplers including annular (Possanzini et al., 1983), coiled (Pui et al., 1990), honeycomb (Koutrakis et al., 1993) and porous metal (Huang et al., 2011; Tsai et al., 2001a, 2003, 2001b) denuders can be used to minimize the positive artifact. For instance, the interfering inorganic basic/acid gases in the air stream can be absorbed by acid/basic coated porous metal discs, respectively, before particle collection by a Teflon filter in the porous metal denuder (Huang et al., 2011; Tsai et al., 2001a, 2001b; 2003). The evaporated fraction from the Teflon filter is collected by the backup filters to correct for the negative artifact. The "actual" $PM_{2.5}$ concentrations are the sum of the $PM_{2.5}$ concentrations measured at the Teflon filter plus the evaporated concentrations obtained from the backup filters (Liu et al., 2014).

The FRM data are not the "true" or "actual" $PM_{2.5}$ but they are the "reference" values to determine the compliance with the NAAQS, and the FRM sampler is often used to evaluate the sampling performance of candidate samplers/monitors. The designation of the FEM monitor requires that the data comparison with the FRM sampler should meet the U.S. EPA criteria with the slope of 1 ± 0.1, the intercept of 0 ± 2 $\mu g\ m^{-3}$, and the regression coefficient (R^2) of ≥ 0.93 (U.S. EPA, 2017a). Two FEM monitors, beta attenuation monitor (BAM) and tapered-element oscillating microbalance with the filter dynamics measurement system (TEOM-FDMS), are widely used for monitoring hourly $PM_{2.5}$ concentrations. The BAM is based on the relationship between the attenuation of the beta ray with the particle deposit on the glass fiber filter (GFF) tape. The BAM (BAM-1020, Met One Instruments Inc.) uses a smart heater which reduces the ambient RH of incoming air to 35% for removing the aerosol water content. It eliminates the positive artifact of water vapor absorption which occurs in the conventional BAM (Chang et al., 2001; Chang and Tsai, 2003; Hauck et al., 2004; Huang and Tai, 2008; Takahashi et al., 2008; Shin et al., 2011; Triantafyllou et al., 2016; Kiss et al., 2017). The comparison of the BAM-1020 with the collocated FRM showed that the BAM-1020 met with the slope (ranging from 0.94 to 1.02) and intercept (ranging from -0.96 to 0.56 $\mu g\ m^{-3}$) criteria of the U.S. EPA and became a FEM-designated monitor (Gobeli et al., 2008). However, in the field comparison, only at 2/3 of 61 U.S. EPA sites that the $PM_{2.5}$ concentrations measured by the BAM-1020, $PM_{2.5,B}$, met the criteria of acceptable slope and intercept (Hanley and Reff, 2011). Higher slopes at the remaining sites were suspected to be due to the smart heater and RH sensor problems during warm seasons. Acid gas absorption by the GFF tape of the BAM-1020 also caused $PM_{2.5}$ over-measurements (Liu et al., 2013).

The TEOM-FDMS is designed to correct for the evaporation loss of SVM by measuring both non-SVM (in the base mode) and SVM (in the reference mode) of $PM_{2.5}$. It uses a Nafion dryer to reduce the RH of incoming airflow to below 10%, which is then heated up to 30 °C before the tapered element to remove the aerosol water content. The $PM_{2.5}$ concentrations of the TEOM-FDMS, $PM_{2.5,T}$, is the sum of non-SVM and SVM. The base mode $PM_{2.5}$ of the TEOM-FDMS is similar to that of the FRM because the evaporation loss of SVM in the former also occurs during sampling (Zhu et al., 2007). The field comparison showed that $PM_{2.5,T}$ was higher than the FRM $PM_{2.5}$ concentrations, $PM_{2.5,FRM}$, and the TEOM-FDMS met the acceptable slope and intercept only at 1/2 and 2/3 of 17 sites, respectively (Hanley and Reff, 2011). Higher $PM_{2.5,T}$ was also reported in previous studies (Grover et al., 2005; Schwab et al., 2006; Zhu et al., 2007; Salvador and Chou, 2014; Liu et al., 2014). The

TEOM-FDMS was found to be more accurate with $PM_{2.5,T}$ approaching the "actual" $PM_{2.5}$ value (Zhu et al., 2007; Liu et al., 2014).

To study the factors affecting the difference in the daily average FEM and FRM measurement values and convert the former to the later, the field comparison between the FEM monitors (BAM-1020 and TEOM-FDMS) and the FRM samplers were conducted. Empirical equations were derived for the conversion of the FEM data to FRM data and the determination of the near "true" or "actual" $PM_{2.5}$ from the FRM $PM_{2.5}$.

2. Materials and methods

Field comparisons between the BAM-1020 (Met One Instruments Inc.) and TEOM-FDMS (1405-F or 1405-DF, Thermo Fisher) monitors and the FRM samplers were conducted at NCTU, Hsinchu (from 18 April to 23 August, 2018) and four Taiwan EPA monitoring stations (from 21 December 2015 to 21 July 2017) two of which were located in northern Taiwan (New Taipei and Taipei cities) and the other two in southern Taiwan (Tainan and Kaohsiung cities) as shown in Fig. 1. At each EPA station, two different seasons were selected including New Taipei winter and summer, Taipei winter and spring, Tainan fall and summer, and Kaohsiung winter and summer. Including NCTU station from spring to summer, there are nine station-seasons with 265 24-hr average samples in total as shown in Table 1. At each EPA station, triplicate FRM (Model PQ-200, BGI), BAM-1020, and TEOM-FDMS (Model 1405-F) were used while at NCTU site, only one FRM (Partisol^{TM} 2000-FRM, Thermo

Fig. 1. Location of all five sampling stations including NCTU, Hsinchu and four Taiwan EPA sampling stations (New Taipei City, Taipei City, Tainan City and Kaohsiung City).

Table 1
The number of daily samples at different stations and seasons.

	NCTU	New Taipei City	Taipei City	Tainan City	Kaohsiung City
Season	spring to summer (18 April – 23 Aug 2018)	spring (05 May - 06 June 2016)	winter (21 Dec 2015–19 Jan 2016)	summer (11 July – 07 Aug 2016)	winter (27 Jan – 29 Feb 2016)
N (samples)	31	29	30	28	30
Season		winter (16 Dec 2016–16 Jan 2017)	spring (13 Mar – 12 April 2016)	fall (01 Sep – 09 Oct 2016)	summer (22 Jun – 21 Jul 2017)
N (samples)		30	30	27	30

Fisher), one BAM-1020, and one TEOM-FDMS (Model 1405-DF) were used. The setup of the FRM samplers, BAM-1020, and TEOM-FDMS are shown in Section S1 in the Supplemental Information (SI). The 24 hourly $PM_{2.5}$ data of the BAM-1020 and TEOM-FDMS were averaged for the comparison with the FRM data. The precision of the triplicate FEM monitors or FRM samplers is calculated as (U.S. EPA, 2017a)

$$Precision\ (\%) = \left(\frac{PM_{2.5,\ max} - PM_{2.5,min}}{PM_{2.5,ave}}\right). \quad (1)$$

where $PM_{2.5,max}$, $PM_{2.5,min}$, and $PM_{2.5,ave}$ are the maximum, minimum, and average values of the triplicate FEM monitors or FEM samplers, respectively. The correlation relationships among triplicate FRM samplers, triplicate BAM-1020 and triplicate TEOM-FDMS was shown in Figs. S1a, S1b, and S1c in Section S2 in the SI, respectively. Three FRM samplers correlate well with each other with good regression parameters and similar results are found for three BAM-1020 and three TEOM-FDMS. The average precision of the 24-hr average $PM_{2.5}$ of the triplicate FRM samplers at all EPA station-seasons was found to be very small, which is only 2%. In comparison, the average precisions of the triplicate BAM-1020 and TEOM-FDMS were somewhat larger, which are 12% and 10%, respectively. This shows that the FRM samplers are much more precise than the FEM monitors.

For the comparison of $PM_{2.5,B}$ or $PM_{2.5,T}$ with $PM_{2.5,FRM}$, the slope, intercept, and correlation coefficient (R^2) of pairwise comparison were determined and compared with the U.S. EPA criteria for class III $PM_{2.5}$ FEM (U.S. EPA, 2017a). The mean normalized bias (MNB) of the 24-hr average $PM_{2.5}$ of the triplicate instruments was also calculated by using Eq. (2) to evaluate the sampling performance of the FEM monitors as follows:

$$\mathrm{MNB}(\%) = \frac{\sum_{i=1}^{N} bias\ (\%)}{N} = \frac{\sum_{i=1}^{N} \frac{\left(PM_{2.5,FEMi} - PM_{2.5,FRMi}\right)}{PM_{2.5,FRMi}}}{N} \times 100\% \quad (2)$$

where bias (%) represents the value of each data point "i", $PM_{2.5,FEMi}$ represents $PM_{2.5,B}$ or $PM_{2.5,T}$ with sample i, and N is the total number of samples at a station at a particular season. The calculated MNB was then compared with the bias criteria, which is less than ±10% for the FEM U.S. EPA, 2017b; Hanley and Reff (2011). Linear regression and ANOVA (analysis of variance) were used to determine whether the $PM_{2.5}$ concentrations, T, and RH affect the differences in the FEM and FRM data. Then, empirical equations were derived for converting the FEM data to FRM data, and the FRM data to the "true" or "actual" $PM_{2.5}$ values. To validate the empirical equations, half data points (133/165 data points) were chosen randomly to derive the equations, which is known as method #1. Then, the derived equations with associated parameters were used to correct for all data points (265 data points). Another method (method #2), in which all data points (265 data points) were used to derive the equations, was then used to justify the validation of the derived empirical equations. The results of method #2 are shown in Section S6 in the SI, and it is found that similar results and empirical equations were obtained.

3. Results and discussion

3.1. Field data comparisons between the FEM monitors and FRM samplers

Fig. 2a and 2b shows the comparison of $PM_{2.5,B}$ and $PM_{2.5,T}$ with $PM_{2.5,FRM}$ at all nine station-seasons, respectively, with a total of 265 data points. $PM_{2.5,FRM}$, T and RH varied from 3.6 to 69.1 $\mu g\ m^{-3}$ (average $PM_{2.5,FRM} = 21.1 \pm 14.7\ \mu g\ m^{-3}$), from 11.5 to 31.4 °C (average T = 24.0 ± 5.2 °C) and from 54.9 to 96.1% (average RH = 78.3 ± 7.6%), respectively, during the test period. The range of $PM_{2.5,FRM}$, T, and RH is wide and the field comparison tests were carried out at five geographically diverse stations at different seasons. The $PM_{2.5}$ chemical

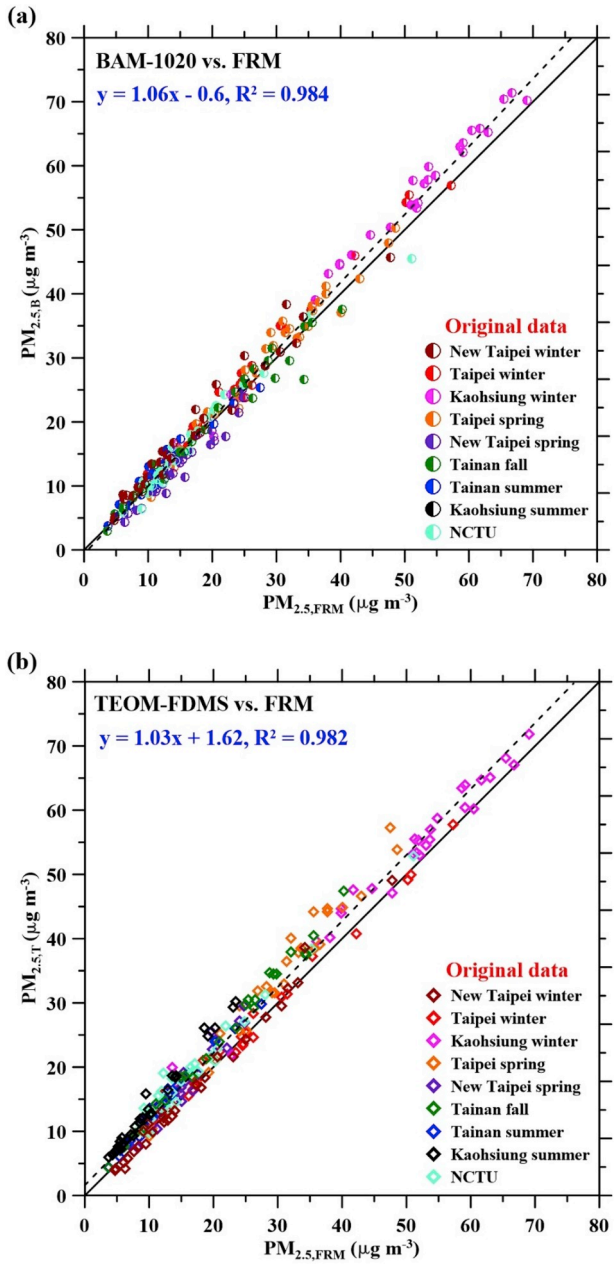

Fig. 2. Correlation plot for (a) $PM_{2.5,B}$ and (b) $PM_{2.5,T}$ verus $PM_{2.5,FRM}$ for all stations and seasons.

composition varies from season to season and site to site in Taiwan, as shown in Section S3 in the SI. In general, the chemical components of $PM_{2.5}$ in different regions in Taiwan are dominant by organic carbon (OC), SO_4^{2-}, NH_4^-, and NO_3^-, which are similar to those in other countries (Cheng and Wang-Li, 2019; Jung et al., 2019; Zhao et al., 2019; T.W. EPA, 2019). Therefore, the findings of this study should be applicable to other parts of the world with ambient conditions similar to this study. The results show that $PM_{2.5,B}$, and $PM_{2.5,T}$ correlate well with $PM_{2.5,FRM}$ with the acceptable criteria of the slope (1 ± 0.1), intercept (0 ± 2 $\mu g\ m^{-3}$), and R^2 (≥0.93) (U.S. EPA, 2017a). $PM_{2.5,B}$ agrees well with $PM_{2.5,FRM}$ with the acceptable criteria at all nine individual station-seasons, while 6 out of 9 station-seasons fail to meet the acceptable criteria for $PM_{2.5,T}$ as shown in Figs. S3 and S4 in Section S4 in the SI.

All BAM-1020 data meet the criteria for the slope, intercept, and R^2 and the MNB of +1.67% also meets the U.S. EPA criteria of ≤±10% bias. However, the standard deviation (SD) of the MNB of ±12.43% is large

with the individual biases varying significantly from −39.53 to +40.98%, as shown in Fig. 3a. In comparison, the MNB of the TEOM-FDMS of +13.86% does not meet the criteria bias with the individual biases varying a lot from −33.33 to +66.32%, as shown in Fig. 3b. In general, the biases of the TEOM-FDMS are always positive for all mass concentration ranges, which is consistent with the previous study (Liu et al., 2014). The biases of the BAM-1020 are positive at the mass concentration higher than 35 $\mu g\ m^{-3}$ and either positive or negative at the mass concentration lower than 35 $\mu g\ m^{-3}$. The MNB is positive at 7 out of 9 station-seasons for the BAM-1020 and 8 out of 9 station-season for the TEOM-FDMS as shown in Tables 2 and 3, respectively. Although the MNB of the BAM-1020 is small, individual station-seasons may have the MNB larger than ±10%. For instance, the BAM-1020 measures slightly 10% more mass than the FRM at New Taipei winter (+11.88 ± 12.08%) and less mass than the FRM at New Taipei spring (−12.41 ± 10.28%) and Kaohsiung summer (−12.81 ± 11.02%). In comparison, at some individual station-seasons, the TEOM-FDMS could measure 10% more mass than the FRM, e.g., at Tainan fall (+18.54 ± 6.90%) and summer (+19.02 ± 6.36%), Kaohsiung summer (+37.15 ± 11.09%), and NCTU (+18.14 ± 13.65%).

It is also seen that the fluctuation of the biases increases with the decreasing $PM_{2.5,FRM}$ for both BAM-1020 (Fig. 3a) and TEOM-FDMS (Fig. 3b). The biases of the BAM-1020 and TEOM-FDMS vary from −11.00 to +13.12% (MNB = +5.10 ± 5.34%) or from −3.32 to +24.16% (MNB = +7.01 ± 6.16%) when $PM_{2.5,FRM}$ is ≥ 35 $\mu g\ m^{-3}$, but they fluctuate significantly from −39.53 to +40.98% (MNB = +0.09 ± 15.48%) or from −33.33 to +66.32% (MNB = +19.31 ± 17.42%), respectively, as $PM_{2.5,FRM}$ is < 15 $\mu g\ m^{-3}$. The differences in $PM_{2.5,B}$ and $PM_{2.5,FRM}$ ($Diff_{B\text{-}FRM}$) and $PM_{2.5,T}$ and $PM_{2.5,FRM}$ ($Diff_{T\text{-}FRM}$) decrease with the increasing $PM_{2.5,FRM}$ and significant bias fluctuation occurs at $PM_{2.5}$ concentrations lower than <15 $\mu g\ m^{-3}$. It is noted that the 24-hr average data of the FEM monitors were averaged from the hourly data, which can be very small at this low concentration range; thus, the bias could be excessive. That is, the current FEM monitors are not able to measure $PM_{2.5}$ concentrations accurately at this low concentration range.

Table 2
The MNB and $Diff_{B\text{-}FRM}$ of original $PM_{2.5,B}$ and converted $PM'_{2.5,B}$.

	MNB (%)		$Diff_{B\text{-}FRM}$ ($\mu g\ m^{-3}$)	
	Original	Converted	Original	Converted
New Taipei winter	+11.88 ± 12.08	+2.47 ± 8.87	+1.55 ± 1.99	+0.03 ± 1.71
New Taipei spring	−12.41 ± 10.28	−6.26 ± 7.65	−1.66 ± 1.32	−0.71 ± 1.26
Taipei winter	+8.91 ± 6.23	+2.09 ± 5.64	+1.83 ± 1.45	+0.15 ± 1.01
Taipei spring	+3.88 ± 8.13	−3.05 ± 5.40	+1.20 ± 1.92	−0.89 ± 1.04
Tainan fall	+1.01 ± 9.62	+3.31 ± 9.85	−0.19 ± 2.08	+0.41 ± 1.79
Tainan summer	+6.95 ± 10.81	+6.28 ± 12.80	+0.66 ± 1.21	+0.63 ± 1.44
Kaohsiung winter	+6.58 ± 5.26	+2.31 ± 5.11	+3.24 ± 1.97	+0.88 ± 1.43
Kaohsiung summer	−12.81 ± 11.02	−3.55 ± 7.17	−0.99 ± 0.84	−0.45 ± 0.92
NCTU	+0.85 ± 9.42	+2.41 ± 7.08	+0.15 ± 1.18	+0.07 ± 0.75
Total	**+1.67 ± 12.43**	**+0.63 ± 8.75**	**+0.66 ± 2.15**	**+0.01 ± 1.47**

Also, it is found that the bias variation of the BAM-1020 and TEOM-FDMS is also affected by ambient conditions. Fig. 4a and 4b shows the relationship of the bias (or difference) with the ambient T for the BAM-

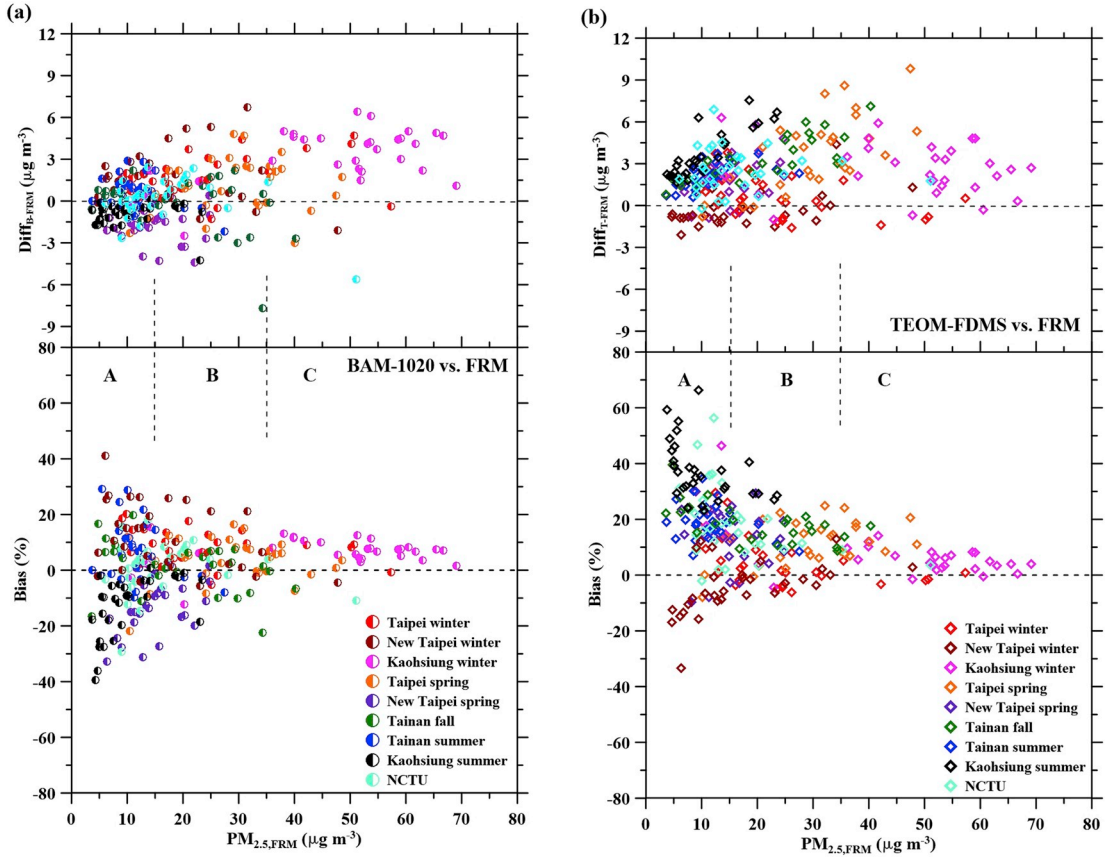

Fig. 3. The relationship of the bias and difference for the (a) BAM-1020 and (b) TEOM-FDMS with $PM_{2.5,FRM}$ for all stations and seasons (Note: A: $PM_{2.5,FRM}$ < 15 $\mu g\ m^{-3}$, B: 15 $\mu g\ m^{-3}$ ≤ $PM_{2.5,FRM}$ < 35 $\mu g\ m^{-3}$, and C: $PM_{2.5,FRM}$ ≥ 35 $\mu g\ m^{-3}$).

Table 3
The MNB and $Diff_{B\text{-}FRM}$ of original $PM_{2.5,T}$ and converted $PM'_{2.5,T}$.

	MNB (%)		$Diff_{T\text{-}FRM}$ ($\mu g\ m^{-3}$)	
	Original	Converted	Original	Converted
New Taipei winter	−4.46 ± 9.74	−5.20 ± 6.72	−0.27 ± 1.25	−0.75 ± 0.99
New Taipei spring	+13.61 ± 10.33	−2.08 ± 8.54	+2.02 ± 1.54	−0.19 ± 1.21
Taipei winter	+5.21 ± 9.39	+2.21 ± 9.57	+0.65 ± 1.46	−0.22 ± 1.78
Taipei spring	+11.09 ± 8.07	+5.50 ± 5.60	+3.58 ± 2.71	+1.66 ± 1.65
Tainan fall	+18.54 ± 6.90	−0.17 ± 4.99	+3.31 ± 1.64	+0.16 ± 0.91
Tainan summer	+19.02 ± 6.36	−6.69 ± 6.31	+2.14 ± 0.85	−0.67 ± 0.61
Kaohsiung winter	+7.12 ± 8.85	−0.52 ± 7.53	+2.57 ± 1.83	−0.80 ± 2.01
Kaohsiung summer	+37.15 ± 11.09	−0.49 ± 11.65	+3.51 ± 1.74	+0.34 ± 1.25
NCTU	+18.14 ± 13.65	−0.61 ± 12.58	+2.48 ± 1.58	−0.17 ± 1.65
Total	**+13.86 ± 14.50**	**−0.85 ± 9.00**	**+2.21 ± 2.07**	**+0.07 ± 1.57**

1020 and TEOM-FDMS, respectively. In general, the bias (or difference) of the BAM-1020 decreases with the increasing T, while that of the TEOM-FDMS increases with the increasing T. When T is lower than 18 °C in winter, $PM_{2.5,B}$ is higher than $PM_{2.5,FRM}$ (MNB = +12.04 ± 7.20%) while $PM_{2.5,T}$ is close to $PM_{2.5,FRM}$ (MNB = +0.4 ± 8.9%). It indicates that the BAM-1020 over-measures $PM_{2.5}$ concentrations compared with both FRM and TEOM-FDMS at T lower than 18 °C. When T is in the range of 18–25 °C in spring and fall, both BAM-1020 and TEOM-FDMS slightly over-measure $PM_{2.5}$ concentrations compared with the FRM with the MNBs of +4.46 ± 9.60% and +6.79 ± 10.85%, respectively. When T is higher than 25 °C in summer, the TEOM-FDMS measures as much as +22.67 ± 12.06% more mass than the FRM, while the BAM-1020 measures either higher or less mass than the FRM with the bias fluctuating from negative value of −39.53% to positive value of +29.09% with a much smaller MNB of −3.39 ± 12.81%.

The difference between $PM_{2.5,T}$ and $PM_{2.5,FRM}$ is due to the evaporation loss while the difference between $PM_{2.5,B}$ and $PM_{2.5,FRM}$ is likely caused by the residual water in the particles, the SVM evaporation loss, and the acid gas absorption by the GFF tape. Therefore, it is clear that the bias (or difference) of $PM_{2.5,T}$ is low (or small) at T lower than 18 °C but becomes positive and larger at T higher than 25 °C due to the increased evaporation loss with the increasing T in the FRM (Wilson et al., 2006). In comparison, the bias (or difference) of $PM_{2.5,B}$ is large at T lower than 18 °C since the water content in particles is not removed completely. As shown in Fig. S6 in the SI, when T is lower than 18 °C and RH and $PM_{2.5,FRM}$ are as high as 81.2 ± 10.6% and 25.6 ± 14.3 $\mu g\ m^{-3}$, respectively, water could be retained easily on the surfaces of particles or trapped physically in the gaps between particles resulting in incomplete removal of water content (Weis et al., 1999; Chang et al., 2003). Another possible explanation is that the ambient RH fluctuates in a wide range in winter at different stations (New Taipei winter: 59.8–90.7%, Taipei winter: 71.0–96.1%, and Kaohsiung winter: 68.2–87.5%), which could cause the hourly RH controlled by the smart heater to lag behind the set point RH of 35% which also results in the incomplete removal of water content.

At T higher than 25 °C, the BAM-1020 is found to under-measure $PM_{2.5}$ concentrations compared to the TEOM-FDMS with the MNB of −20.43 ± 13.09% indicating that the BAM-1020 has the evaporation loss. Moreover, the evaporation loss in the BAM-1020 is higher than that in the FRM, resulting in the under-measurement of the BAM-1020. It is

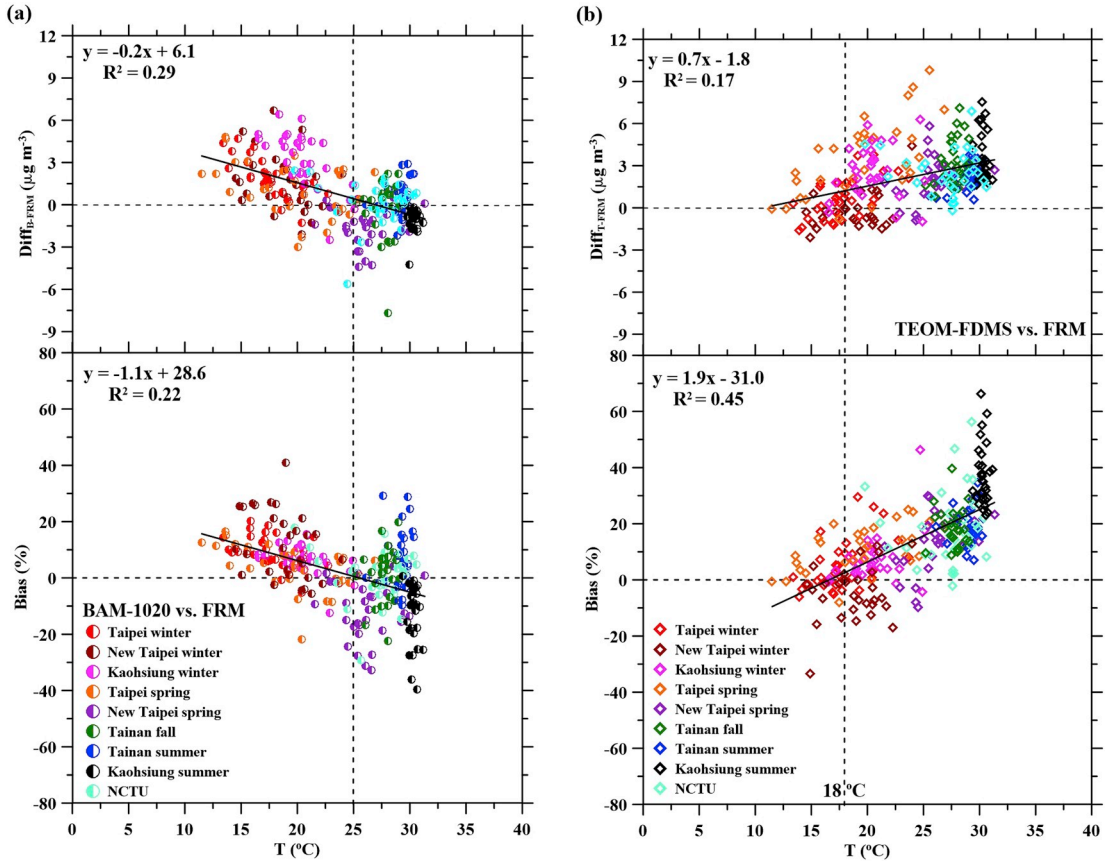

Fig. 4. The relationship of the bias and $Diff_{B\text{-}FRM}$ for the (a) BAM-1020 and (b) TEOM-FDMS with the ambient T for all stations and seasons.

because that at this higher temperature condition, the average RH and $PM_{2.5,FRM}$ are 76.3 ± 5.8% and 14.6 ± 8.5 $\mu g\ m^{-3}$, respectively, which are not as high as those at the lower temperature condition of 18 °C discussed in the above paragraph, the heated temperature by the smart heater becomes higher (higher heating power) and causes more evaporation loss of SVMs (Khlystov et al., 2005; Zhu et al., 2007). The heated temperature and the WVC (water vapor concentration) difference before and after the smart heater at different ambient conditions are shown in Section S5 in the SI to help elucidate why the BAM-1020 has higher evaporation loss at T > 25 °C. Moreover, the reduction of aerosol water content can cause the evaporation loss of water-soluble organic matter (WSOM) in particles (El-Sayed et al., 2016). Whereas, the BAM-1020 also over-measures $PM_{2.5}$ concentrations at Tainan fall and summer and NCTU at this temperature condition likely due to the acid gas absorption by the GFF tape of the BAM-1020 (Liu et al., 2013). Besides, it is found that the smart heater cannot control the RH to the set point of 35%, and the hourly controlled RH increases with the increasing ambient RH as shown in Fig. S7 in the SI, using the NCTU station as an example, which also results in incomplete removal of aerosol water content and over-measurement $PM_{2.5}$.

3.2. Conversion of the FEM $PM_{2.5}$ concentration

To reduce the observed differences between the FEM and FRM values, the linear regression and ANOVA were used to determine whether $Diff_{B–FRM}$ or $Diff_{T–FRM}$ ($\mu g\ m^{-3}$) are affected by $PM_{2.5}$ concentrations, T, or RH. Then the empirical equations were derived accordingly to convert the FEM data to the FRM data. The results show that $Diff_{B–FRM}$ is affected significantly by $PM_{2.5,B}$ (p-value < 0.001), T (p-value < 0.001), or RH (p-value < 0.05) but only $PM_{2.5,B}$ and T show a linear regression relationship with $Diff_{B–FRM}$ with R^2 of 0.29 and 0.3, respectively. The linear regression relationship of $Diff_{B–FRM}$ with T, RH, and $PM_{2.5,B}$ is improved by different combinations of T, RH, and $PM_{2.5,B}$ at different conditions as shown in Table 4. Fig. 5 shows that the bias and $Diff_{B-FRM}$ have a better linear relationship with the combined parameter of T*RH*0.01 with the R^2 of 0.3 for the bias and 0.42 for $Diff_{B-FRM}$ as compared to that based on T as the parameter. It indicates that the effects of these parameters on the differences between the FEM data and the FRM data are inter-dependent. It is found that $Diff_{B-FRM}$ is positive (+1.13 ± 2.11 $\mu g\ m^{-3}$) and decreases linearly with the increasing combined parameter of T*RH*0.01 and the decreasing $PM_{2.5,B}$ when T is lower than 25 °C regardless of RH or T is higher than 25 °C, but RH is lower than 75% (p-value < 0.001 and $R^2 = 0.51$). However, when T and RH are high (T ≥ 25 °C and RH ≥ 75%), $Diff_{B-FRM}$ is found to be affected significantly by T*RH*0.01 (p-value < 0.05) but the linear relationship is not good ($R^2 = 0.1$). Also, $Diff_{B-FRM}$ is not affected by $PM_{2.5,B}$ (p-value = 0.16) at this high T and RH condition.

It is found that when T and RH are higher than 25 °C and 75%, respectively, the linear relationship of $Diff_{B-FRM}$ with the T, RH, and $PM_{2.5,B}$ is complicated and depends strongly on different combined parameters within different $PM_{2.5,B}$ range. When $PM_{2.5,B}$ is lower than 10 $\mu g\ m^{-3}$, and T varies from 25 to 27 °C, $Diff_{B-FRM}$ is negative (−1.32 ± 1.44 $\mu g\ m^{-3}$) and decreases linearly with the decreasing T*RH*0.01 and the increasing $PM_{2.5,B}$ (p-value < 0.05 and $R^2 = 0.36$). Similarly, when $PM_{2.5,B}$ is lower than 10 $\mu g\ m^{-3}$ but T is higher than 27 °C, $Diff_{B-FRM}$ is close to zero (+0.00 ± 1.41 $\mu g\ m^{-3}$) and decreases linearly with the decreasing T*RH*0.01 and the increasing $PM_{2.5,B}$ (p-value < 0.05 and $R^2 = 0.46$). On the other hand, when $PM_{2.5,B}$ is higher than 10 $\mu g\ m^{-3}$, $Diff_{B-FRM}$ is not a function of T*RH*0.01 and $PM_{2.5,B}$. In this mass concentration range, $Diff_{B-FRM}$ decreases linearly with the decreasing T and the increasing T*RH*0.01 when $PM_{2.5,B}$ is in the range of 10–20 $\mu g\ m^{-3}$ (p-value < 0.001 and $R^2 = 0.36$) and higher than 20 $\mu g\ m^{-3}$ (p-value < 0.006 and $R^2 = 0.40$), respectively, as shown in Table 4.

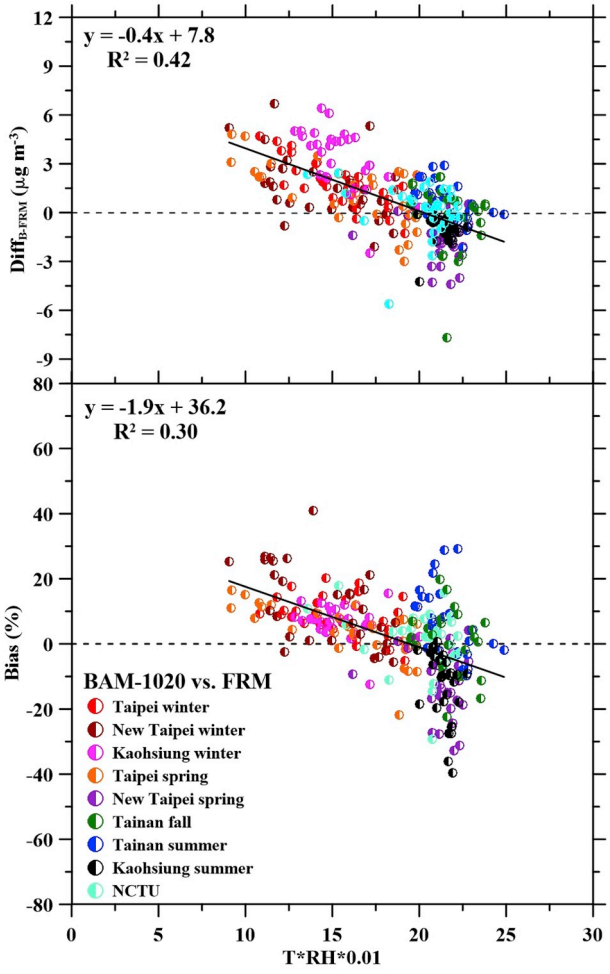

Fig. 5. The relationship of the bias and $Diff_{B-FRM}$ with the combined parameter of T*RH*0.01 for all stations and seasons.

As discussed in Section 3.1, at the temperature lower than 18 °C, the aerosol water content cannot be removed completely such that most of $PM_{2.5,B}$ are higher than $PM_{2.5,FRM}$. That is, $Diff_{B-FRM}$ is influenced by T, RH, and $PM_{2.5,B}$. When T is higher than 25 °C, but RH is lower than 75%, $PM_{2.5,B}$ is just slightly lower than $PM_{2.5,FRM}$ with the average $Diff_{B-FRM}$ (MNB) of −0.15 ± 1.36 $\mu g\ m^{-3}$ (−6.30 ± 16.85%) since the aerosol water content can be removed completely (Chang et al., 2003). On the other hand, heating the aerosol by the smart heater to remove the

Table 4
The linear regression relationship of $Diff_{B-FRM}$ with T, RH and $PM_{2.5,B}$ at different conditions.

Parameters	T (°C)	RH (%)	$PM_{2.5,B}$ ($\mu g\ m^{-3}$)	N[a]	R^2	p-value
$\frac{PM_{2.5,B}}{T \times RH \times 0.01}$	<25	-	-	130	0.51	<0.001
	≥25	<75	-	61		
	25–27	≥75	<10	11	0.36	0.04
	≥27			12	0.46	0.01
T			10–20	33	0.36	<0.001
T × RH × 0.01			≥20	18	0.40	0.006

[a] N is the number of data point (ΣN = 265).

aerosol water content at T higher than 25 °C and RH higher than 75% may cause over-measurement or sometimes under-measurement due to the complicated evaporation loss and incomplete removal of aerosol water content, and possible acid gas adsorption as discussed above.

Based on the linear regression relationship of $Diff_{B\text{-}FRM}$ ($\mu g\ m^{-3}$) with T (°C), RH (%), and $PM_{2.5,B}$ ($\mu g\ m^{-3}$), the empirical equations were derived to convert $PM_{2.5,B}$ to $PM_{2.5,FRM}$ as

$$PM'_{2.5,B} = PM_{2.5,B} - Diff_{B\text{-}FRM} \quad (3)$$

where $PM'_{2.5,B}$ is the converted $PM_{2.5}$ of the BAM-1020 to $PM_{2.5,FRM}$ with $Diff_{B\text{-}FRM}$ calculated as

$$Diff_{B-FRM} = \alpha \frac{PM_{2.5,B}{}^{\beta}}{T \times RH \times 0.01} + \gamma \quad (4)$$

$$= \alpha \times T + \gamma \quad (5)$$

$$= \alpha \times T \times RH \times 0.01 + \gamma \quad (6)$$

where α, β, and γ are empirical parameters given in Table 5 at different ranges of T, RH, and $PM_{2.5,B}$. Half data points (133/265 data points) were chosen randomly to determine the empirical equations, and all data points (265 data points) were corrected by using Eqs. (3)–(6). After correction, the MNB ($Diff_{B\text{-}FRM}$) is decreased from +1.67 ± 12.43% (+0.66 ± 2.15 $\mu g\ m^{-3}$) to +0.63 ± 8.75% (+0.01 ± 1.47 $\mu g\ m^{-3}$) for all $PM_{2.5}$ data from 9 station-seasons. The MNBs of all individual station-seasons shown in Table 2 are improved and meet the U.S. EPA criteria with a bias of ≤±10% (U.S. EPA, 2017b). The linear regression parameters of the converted $PM'_{2.5,B}$, and $PM_{2.5,\ FRM}$ are also improved as shown in Fig. 6a. It indicates that the derived empirical equations can be used to correct for the difference and convert the $PM_{2.5}$ of the BAM-1020 as the FRM $PM_{2.5}$ with good accuracy.

The relationship between $Diff_{T\text{-}FRM}$ with T, RH, and $PM_{2.5,T}$ was also studied and the results show that $Diff_{T\text{-}FRM}$ is also affected significantly by T (p-value < 0.001), RH (p-value < 0.001), and $PM_{2.5,T}$ (p-value < 0.001) but without good linear relationship (R^2 is 0.17 for the T, 0.006 for the RH, and 0.1 for the $PM_{2.5,T}$). The RH has no linear regression relationship with $Diff_{T\text{-}FRM}$ since RH of the incoming aerosol flow in the TEOM-FDMS is decreased to less than 10% by the Nafion drier to ensure no aerosol water content exists. It is found that $Diff_{B\text{-}FRM}$ shows a good linear relationship with T^2 and $PM_{2.5,T}$ at the 99% confidence interval (p-value < 0.001 and $R^2 = 0.42$). Therefore, $PM_{2.5,T}$ can be converted to $PM_{2.5,FRM}$ by the following equation:

$$PM'_{2.5,T} = PM_{2.5,T} - Diff_{T\text{-}FRM} \quad (7)$$

where $PM'_{2.5,T}$ is the converted $PM_{2.5}$ of the TEOM-FDMS to $PM_{2.5,FRM}$ with $Diff_{T\text{-}FRM}$ fitted as

$$Diff_{T\text{-}FRM} = \alpha\ T^2 + \beta\ PM_{2.5,T} + \gamma \quad (8)$$

where the empirical parameters α, β, and γ are 0.0052, 0.078, and −2.68, respectively, which were determined using method #1 (half data points of 133/265 were used). The converted $PM'_{2.5,T}$ are close to the FRM $PM_{2.5}$ with the MNB ($Diff_{T\text{-}FRM}$) reduced from 13.86 ± 14.50% (+2.21 ± 2.07 $\mu g\ m^{-3}$) to −0.85 ± 9.0% (−0.07 ± 1.57 $\mu g\ m^{-3}$). It is seen that the individual MNB and $Diff_{T\text{-}FRM}$ are also improved and meet the U.S. EPA criteria for all stations at all seasons as shown in Table 3 resulting in the improvement of the linear regression parameters of the converted $PM'_{2.5,T}$ and $PM_{2.5,FRM}$ as shown in Fig. 6b. Unlike BAM-1020, only one empirical equation without the parameter RH is needed to convert $PM_{2.5,T}$ to $PM_{2.5,FRM}$, while three empirical equations are needed for the conversion of the $PM_{2.5,B}$ because aerosol heating method to eliminate aerosol water content also likely induce evaporation loss of

Table 5
The values of empirical parameters of Eqs. (4)–(6).

	T (°C)		RH (%)	$PM_{2.5,B}$ ($\mu g\ m^{-3}$)	α	β	γ
[a] Eq. (4)	<25		-	-	32.03	0.25	−3.08
	≥25		<75	-			
		25–27	≥75	<10	−120.98	0.25	6.89
		≥27			−159.89	0.25	12.10
[b] Eq. (5)				10–20	0.64	-	−17.90
[c] Eq. (6)				≥20	−3.41	-	74.01

[a] $Diff_{B\text{-}FRM} = \alpha \frac{PM_{2.5,B}^{\beta}}{T \times RH \times 0.01} + \gamma$.
[b] $Diff_{B\text{-}FRM} = \alpha \times T + \gamma$; and.
[c] $Diff_{B\text{-}FRM} = \alpha \times T \times RH \times 0.01 + \gamma$.

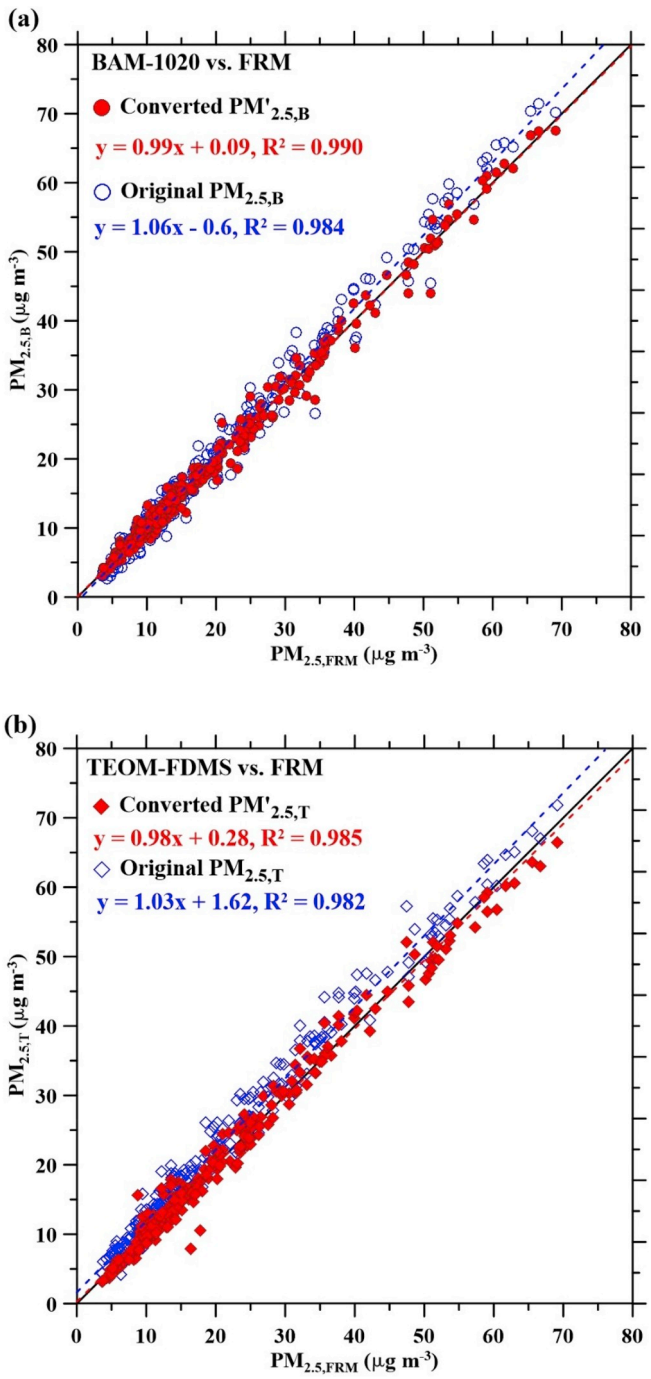

Fig. 6. Correlation plot for the converted (a) $PM'_{2.5,B}$ and (b) $PM'_{2.5,T}$ versus $PM_{2.5,FRM}$ for all stations and seasons.

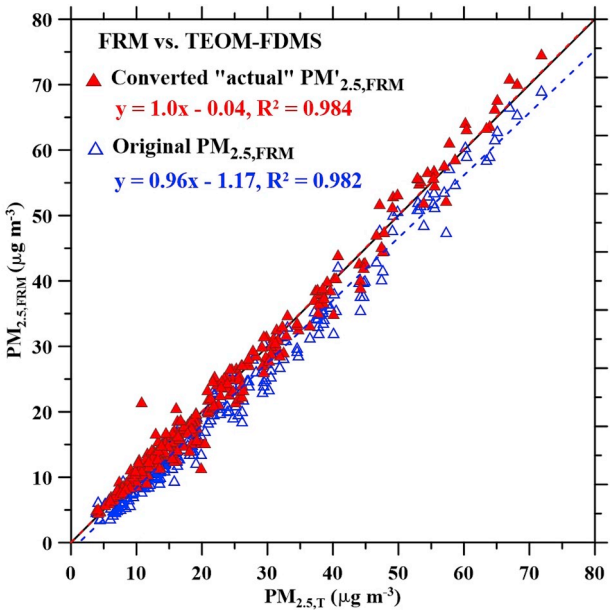

Fig. 7. Correlation plot for the converted "actual" $PM'_{2.5,FRM}$ versus $PM_{2.5,T}$ for all stations and seasons.

SVM and incomplete removal of aerosol water in some cases. In summary, after correction, most of the daily average data of the BAM-1020 and TEOM-FDMS meet the U.S. EPA criteria for the bias smaller than ±10%. Only 63 out of 265 data (or 24%) of the BAM-1020 and 61 out of 265 data (or 23%) have biases greater than 10%, which is a good improvement over the uncorrected values with 97 out of 265 data (37%) for the BAM-1020 and 130 out of 265 data (or 49%) for the TEOM-FDMS. The precisions between three identical BAM-1020 and three TEOM-FDMS determined in this study are 12% and 10%, respectively, which are much higher than the precision of 2% for the three identical FRM which explains the reason why the biases of some converted values still exceed 10%. The correlation relationships of the data of the individual BAM-120 and individual TEOM-FDMS with the average FRM data are shown in Section 7 in the SI. The results show that the bias (or difference) for the individual BAM-1020 and TEOM-FDMS are all improved after correction.

3.3. *"Actual" $PM_{2.5}$ converted from the FRM*

The FRM has a negative artifact due to the evaporation loss, which causes the under-measured $PM_{2.5}$. Therefore, the FRM $PM_{2.5}$ is not an "actual" $PM_{2.5}$. The TEOM-FDMS corrects for the evaporation loss and has been shown to measure the accurate $PM_{2.5}$. In the previous section, the empirical equation was derived to convert $PM_{2.5,T}$ to the FRM $PM'_{2.5,T}$ for the TEOM-FDMS. Since the difference between $PM_{2.5,T}$ and $PM_{2.5,FRM}$ is found to be influenced by T^2 and $PM_{2.5,T}$ and can be fitted by using Eq. (8), the near "true" or "actual" $PM_{2.5}$ of the FRM, $PM'_{2.5,FRM}$, which is assumed to be equal to $PM_{2.5,T}$, can be calculated as

$$PM'_{2.5,FRM} = PM_{2.5,T} = \frac{PM_{2.5,FRM} + \alpha T^2 + \gamma}{1-\beta} \quad (9)$$

Since Eq. (9) is the re-arrangement of Eq. (8), the empirical parameters α, β, and γ are 0.0052, 0.078, and −2.68, respectively, which are the same as those in Eq. (8). After correction, the MNB ($Diff_{FRM-T}$) of the converted "actual" $PM_{2.5}$ is reduced substantially from −10.76 ± 11.42% (−2.21 ± 2.07 μg m^{-3}) to +1.33 ± 8.44% (+0.08 ± 1.70 μg m^{-3}), and the converted FRM $PM_{2.5}$ correlate well with the TEOM-FDMS $PM_{2.5}$ with the improve regression parameters as shown in Fig. 7. The individual MNB and $Diff_{FRM-T}$ at different stations and seasons shown in Table S7 in the SI show that the converted "actual" $PM_{2.5}$ concentrations of the FRM are very close to those of the TEOM-FDMS. That is, the derived empirical equation can be used to determine the near "actual" $PM_{2.5}$ values when only FRM data are available.

4. Conclusions

The present study conducted the field comparison test of the automated FEM monitors (BAM-1020 and TEOM-FDMS) with the manual FRM samplers. Although the $PM_{2.5}$ concentrations of the BAM-1020 are comparable to those of the FRM with acceptable slopes (1 ± 0.1) and intercepts (0 ± 2 μg m^{-3}) and R^2 of >0.93 at 9 out of 9 station-seasons, the biases do not meet the U.S. EPA criteria (bias ≤ ±10%). The BAM-1020 over-measures $PM_{2.5}$ at the temperature lower than 18 °C and either over-measures or under-measures $PM_{2.5}$ at the temperature higher than 25 °C due to aerosol water content and acid gas absorption or evaporation loss, respectively. In comparison, the $PM_{2.5}$ concentrations of the TEOM-FDMS are comparable to those of the FRM at only 3 out of 9 station-seasons. The TEOM-FDMS always over-measures $PM_{2.5}$ due to evaporation loss in FRM $PM_{2.5}$, which is increased with the increasing temperature. The differences between FEM and FRM values can be corrected by using the empirical equations when the temperature, relative humidity, and $PM_{2.5}$ concentrations are known. The FEM $PM_{2.5}$ are close to the FRM $PM_{2.5}$ after conversion with the average bias less than ±10% for all stations and seasons, and the FRM $PM_{2.5}$ can also be converted to the nearly "actual" $PM_{2.5}$ of the TEOM-FDMS. The derived empirical equations should also be applicable in many parts of the world that have similar ambient conditions to this study.

Declaration of competing interest

The authors declare that they have no known competing financial interests or personal relationships that could have appeared to influence the work reported in this paper.

Acknowledgments

The authors gratefully acknowledge financial support from the Taiwan Ministry of Science and Technology via the contracts MOST 108-2622-8-009-012-TE5, 107-3011-F-009-002- and 107-2221-E-009-004-MY3, and the Higher Education Sprout Project of the National Chiao Tung University and Ministry of Education, Taiwan.

Appendix A. Supplementary data

Supplementary data to this article can be found online at https://doi.org/10.1016/j.atmosenv.2019.117138.

References

Bai, L., Huang, L., Wang, Z.L., Ying, Q., Zheng, J., Shi, X.W., Hu, J.L., 2019. Long-term field evaluation of low-cost particulate matter sensors in Nanjing. Aerosol Air Qual. Res. https://doi.org/10.4209/aaqr.2018.11.0424.

Chang, C.T., Tsai, C.J., 2003. A model for the relative humidity effect on the readings of the PM_{10} beta-gauge monitor. J. Aerosol Sci. 34, 1685–1697. https://doi.org/10.1016/S0021-8502(03)00356-2.

Chang, C.T., Tsai, C.J., Lee, C.T., Chang, S.Y., Cheng, M.T., Chein, H.M., 2001. Differences in PM_{10} concentrations measured by beta-gauge monitor and hi-vol sampler. Atmos. Environ. 35, 5741–5748. https://doi.org/10.1016/S1352-2310(01)00369-7.

Cheng, Y.H., Tsai, C.J., 1997. Evaporation loss of ammonium nitrate particles during filter sampling. J. Aerosol Sci. 28, 1553–1567. https://doi.org/10.1016/S0021-8502(97)00033-5.

Cheng, B., Wang-Li, L., 2019. Spatial and temporal variations of PM2.5 in North Carolina. Aerosol Air. Qual. Res. 19 (4), 698–710. https://doi.org/10.4209/aaqr.2018.03.0111.

El-Sayed, M.M.H., Amenumey, D., Hennigan, C.J., 2016. Drying induced evaporation of secondary organic aerosol during summer. Environ. Sci. Technol. 50, 3626–3633. https://doi.org/10.1021/acs.est.5b06002.

EPA, T.W., 2019. $PM_{2.5}$ chemical composition. https://airtw.epa.gov.tw/CHT/TaskMonitoring/Chemical/MonitoringData.aspx. Access date: 04/11/2019.

Gobeli, D., Schloesser, H., PottbergMet, T., 2008. Met one instruments BAM-1020 beta attenuation mass monitor US-EPA PM2.5 federal equivalent method field test results. Paper #2008-A-485-AWMA. http://citeseerx.ist.psu.edu/viewdoc/download?doi=10.1.1.584.2489&rep=rep1&type=pdf.

Grover, B.D., Kleinman, M., Eatough, N.L., Eatough, D.J., Hopke, P.K., Long, R.W., Wilson, W.E., Meyer, M.B., Ambs, J.L., 2005. Measurement of total $PM_{2.5}$ mass (nonvolatile plus semi volatile) with the filter dynamic measurement system tapered element oscillating microbalance monitor. J. Geophys. Res. 110, D07S03. https://doi.org/10.1029/2004JD004995.

Grover, B.D., Kleinman, M., Eatough, N.L., Eatough, D.J., Cary, R.A., Hopke, P.K., Wilson, W.E., 2008. Measurement of fine particulate matter nonvolatile and semi-volatile organic material with the sunset laboratory carbon aerosol monitor. J. Air Waste Manag. Assoc. 58, 72–77. https://doi.org/10.3155/1047-3289.58.1.72.

Hanley, T., Reff, A., 2011. Assessment of PM2.5 FEMs Compared to Collocated FRMs. EPA, U.S. https://www3.epa.gov/ttnamti1/files/ambient/pm25/HanleyandReff040711.pdf.

Hauck, H., Berner, A., Gomiscek, B., Stopper, S., Puxbaum, H., Preining, O., Kundi, M., 2004. On the equivalence of gravimetric PM data with TEOM and beta attenuation measurements. J. Aerosol Sci. 35, 1135–1149. https://doi.org/10.1016/j.jaerosci.2004.04.004.

Huang, C.H., Tai, C.Y., 2008. Relative humidity effect on $PM_{2.5}$ reading recorded by collocated beta attenuation monitors. Environ. Eng. Sci. 25, 1079–1089. https://doi.org/10.1089/ees.2007.0142.

Huang, C.H., Tsai, C.J., Shih, T.S., 2011. Particle collection efficiency of an inertial impactor with porous metal substrates. J. Aerosol Sci. 32 (9), 1035–1044. https://doi.org/10.1016/S0021-8502(01)00038-6.

Johnson, K.K., Bergin, M.H., Russell, A.G., Hagler, G.S.W., 2018a. Field test of several low-cost particulate matter sensors in high and low concentration urban environments. Aerosol Air Qual. Res. 18, 565–578. https://doi.org/10.4209/aaqr.2017.10.0418.

Johnson, N.E., Bonczak, B., Kontokosta, C.E., 2018b. Using a gradient boosting model to improve the performance of low-cost aerosol monitors in a dense, heterogeneous urban environment. Atmos. Environ. https://doi.org/10.1016/j.atmosenv.2018.04.019.

Jung, J., Ghim, Y.S., Lyu, Y.S., Lim, Y., Park, J., Sung, M., 2019. Quantification of regional contributions to fine particles at downwind areas under Asian continental outflows during winter 2014. Atmos. Environ. 210, 231–240. https://doi:10.1016/j.atmosenv.2019.04.062.

Kenny, L.C., Thorpe, A., Stacey, P., 2017. A collection of experimental data for aerosol monitoring cyclones. Aerosol Sci. Technol. 51 (10), 1190–1200. https://doi.org/10.1080/02786826.2017.1341620.

Khlystov, A., Stanier, C.O., Takahama, S., Pandis, S.N., 2005. Water content of ambient aerosol during the Pittsburgh air quality study. J. Geophys. Res. 110, D07S10. https://doi.org/10.1029/2004JD004651.

Kiss, G., Imre, K., Molnár, Á., Gelencsér, A., 2017. Bias caused by water adsorption in hourly PM measurements. Atmos. Meas. Technol. 10, 2477–2484. https://doi.org/10.5194/amt-10-2477-2017.

Koutrakis, P., Sioutas, C., Ferguson, S.T., Wolfson, J.M., Mulik, J.D., Burton, R.M., 1993. Development and evaluation of a glass Honeycomb denuder filter pack system to collect atmospheric gases and particles. Environ. Sci. Technol. 27, 2497–2501. https://doi.org/10.1021/es00048a029.

Kuula, J., Kuuluvainen, H., Rönkkö, T., Niemi, J.V., Saukko, E., Portin, H., Aurela, M., Saarikoski, S., Rostedt, A., Hillamo, R., Timonen, H., 2019. Applicability of optical and diffusion charging-based particulate matter sensors to urban air quality measurements. Aerosol Air Qual. Res. https://doi.org/10.4209/aaqr.2018.04.0143.

Le, T.C., Tsai, C.J., 2017. Novel non-bouncing $PM_{2.5}$ impactor modified from well impactor ninety-six. Aerosol Sci. Technol. 51 (11), 1287–1295. https://doi.org/10.1080/02786826.2017.1341621.

Le, T.C., Shukla, K.K., Sung, J.C., Li, Z.Y., Yeh, H.J., Huang, W., Tsai, C.J., 2019. Sampling efficiency of low-volume PM_{10} inlets with different impaction substrates. Aerosol Sci. Technol. https://doi.org/10.1080/02786826.2018.1559919.

Liu, C.N., Chen, S.C., Tsai, C.J., 2011. A novel multifilter PM_{10}–$PM_{2.5}$ sampler (MFPPS). Aerosol Sci. Technol. 45, 1480–1487. https://doi.org/10.1080/02786826.2011.602135.

Liu, C.N., Awasthi, A., Hung, Y.H., Gugamsetty, B., Tsai, C.J., Wu, Y.C., Chen, C.F., 2013. Difference in 24-h average $PM_{2.5}$ concentrations between the beta attenuation monitor (BAM) and the dichotomous sampler (Dichot). Atmos. Environ. 75, 341–347. https://doi.org/10.1016/j.atmosenv.2013.04.062.

Liu, C.N., Lin, S.F., Awasthi, A., Tsai, C.J., 2014. Sampling and conditioning artifacts of $PM_{2.5}$ in filter-based samplers. Atmos. Environ. 85, 48–53. https://doi.org/10.1016/j.atmosenv.2013.11.075.

Liu, C.N., Lin, S.F., Tsai, C.J., Wu, Y.C., Chen, C.F., 2015. Theoretical model for the evaporation loss of $PM_{2.5}$ during filter sampling. Atmos. Environ. 109, 79–86. https://doi.org/10.1016/j.atmosenv.2015.03.012.

Ly, B.T., Matsumi, Y., Nakayama, T., Sakamoto, Y., Kajii, Y., Nghiem, T.D., 2018. Characterizing $PM_{2.5}$ in Hanoi with new high temporal resolution sensor. Aerosol Air Qual. Res. 18, 2487–2497. https://doi.org/10.4209/aaqr.2017.10.0435.

Malm, W.C., Schichtel, B.A., Pitchford, M.L., 2011. Uncertainties in $PM_{2.5}$ gravimetric and speciation measurements and what we can learn from them. J. Air Waste Manag. 61, 1131–1149. https://doi.org/10.1080/10473289.2011.603998.

Mauderly, J.L., Samet, J.M., 2009. Is there evidence for synergy among air pollutants in causing health effects? Environ. Health Perspect. 117 (1), 1–6. https://doi.org/10.1289/ehp.11654.

Noble, C.A., Vanderpool, R.W., Peters, T.M., McElroy, F.F., Gemmill, D.B., Wiener, R.W., 2001. Federal reference and equivalent methods for measuring fine particulate matter. Aerosol Sci. Technol. 34, 457–464. https://doi.org/10.1080/02786820121582.

Peters, T.M., Vanderpool, R.W., Wiener, R.W., 2001. Design and calibration of the EPA $PM_{2.5}$ well impactor ninety-six (WINS). Aerosol Sci. Technol. 34, 389–397. https://doi.org/10.1080/02786820120352.

Possanzini, M., Febo, A., Liberti, A., 1983. New design of a high-performance denuder for the sampling of atmospheric pollutants. Atmos. Environ. 17, 2605–2610. https://doi.org/10.1016/0004-6981(83)90089-6.

Pui, D.Y.H., Lewis, C.W., Tsai, C.J., Liu, B.Y.H., 1990. A compact coiled denuder for atmospheric sampling. Environ. Sci. Technol. 24 (3), 307–312. https://doi.org/10.1021/es00073a003.

Salvador, C.M., Chou, C.C., 2014. Analysis of semi-volatile materials (SVM) in fine particulate matter. Atmos. Environ. 95, 288–295. https://doi.org/10.1016/j.atmosenv.2014.06.046.

Schwab, J.J., Felton, H.D., Rattigan, O.V., Demerjian, K.L., 2006. New York state urban and rural measurements of continuous $PM_{2.5}$ mass by FDMS, TEOM, and BAM. J. Air Waste Manag. Assoc. 56, 372–383. https://doi.org/10.1080/10473289.2006.10464523.

Seinfield, J.H., Pandis, S.N., 2006. Atmospheric Chemistry and Physics: from Air Pollution to Climate Change, second ed.s. John Wiley & Sons, Inc., New Jersey.

Shin, S.E., Jung, C.H., Kim, Y.P., 2011. Analysis of the measurement difference for the PM_{10} concentrations between beta-ray absorption and gravimetric methods at Gosan. Aerosol Air Qual. Res. 11, 846–853. https://doi.org/10.4209/aaqr.2011.04.0041.

Steinle, S., Reis, S., Sabel, C.E., 2013. Quantifying human exposure to air pollution–moving from static monitoring to spatio-temporally resolved personal exposure assessment. Sci. Total Environ. 443, 184–193. https://doi.org/10.1016/j.scitotenv.2012.10.098.

Takahashi, K., Minoura, H., Sakamoto, K., 2008. Examination of discrepancies between beta-attenuation and gravimetric methods for the monitoring of particulate matter. Atmos. Environ. 42 (21), 5232–5240. https://doi.org/10.1016/j.atmosenv.2008.02.057.

Tolocka, M.P., Peters, T.M., Vanderpool, R.W., Chen, F.L., Wiener, R.W., 2001. On the modification of the low flow-rate PM_{10} dichotomous sampler inlet. Aerosol Sci. Technol. 34, 407–415. https://doi.org/10.1080/02786820119350.

Triantafyllou, E., Diapouli, E., Tsilibari, E.M., Adamopoulos, A.D., Biskos, G., Eleftheriadi, K., 2016. Assessment of factors influencing PM mass concentration measured by gravimetric & beta attenuation techniques at a suburban site. Atmos. Environ. 131, 409–417. https://doi.org/10.1016/j.atmosenv.2016.02.010.

Tsai, C.J., Huang, C.H., Wang, S.H., Shih, T.S., 2001a. Design and testing of a porous metal denuder. Aerosol Sci. Technol. 35, 611–616. https://doi.org/10.1080/02786820117809.

Tsai, C.J., Huang, C.H., Wang, S.H., 2001b. Collection efficiency and capacity of three samplers for acidic and basic gases. Environ. Sci. Technol. 35, 2572–2575. https://doi.org/10.1021/es001943z.

Tsai, C.J., Huang, C.H., Lin, Y.C., Shih, T.S., Shih, B.H., 2003. Field test of a porous metal denuder sampler. Aerosol Sci. Technol. 37, 967–974. https://doi.org/10.1080/02786820300901.

Tsyro, S.G., 2005. To what extent can aerosol water explain the discrepancy between model calculated and gravimetric PM10 and PM2.5? Atmos. Chem. Phys. 5, 515–532. https://doi.org/10.5194/acpd-4-6025-2004.

U.S. EPA, 2016. Monitoring $PM_{2.5}$ in ambient air using designated reference or class I equivalent methods. In: Quality Assurance Handbook for Air Pollution Measurement Systems, vol. II, pp. 2–12. Part II, Section. https://www3.epa.gov/ttnamti1/files/ambient/pm25/qa/m212.pdf.

U.S. EPA, 2017. Ambient Air Monitoring Reference and Equivalent Methods. 40 CFR, Part 53, Federal Code of Regulations. U.S. Government Printing Office, Washington, D.C.

U.S. EPA, 2017. Quality Assurance Requirements for Monitors Used in Evaluations of National Ambient Air Quality Standards. 40 CFR, Part 58, Federal Code of Regulations. U.S. Government Printing Office, Washington, D.C.

Watson, J.G., Tropp, R.J., Kohl, S.D., Wang, X.L., Chow, J.C., 2017. Filter processing and gravimetric analysis for suspended particulate matter samples. Aerosol Sci. Eng. 1−13 https://doi.org/10.1007/s41810-017-0010-4.

Weis, D.D., Ewing, G.E.J., 1999. Water content and morphology of sodium chloride aerosol particles. Geophys. Res. 104, 21275–21285. https://doi.org/10.1029/1999JD900286.

Wilson, W.E., Grover, B.D., Long, R.W., Eatough, N.L., Eatough, D.J., 2006. The measurement of fine particulate semivolatile material in urban aerosols. J. Air Waste Manag. Assoc. 56 (4), 384–397. https://doi.org/10.1080/10473289.2006.10464527.

Zhao, L., Wang, L., Tan, J., Duan, J., Ma, X., Zhang, C., Ji, S., Qu, M., Lu, X.H., Wang, Y., Wang, Q., Xu, R., 2019. Changes of chemical composition and source apportionment of PM2.5 during 2013–2017 in urban Handan, China. Atmos. Environ. Times 206, 119–131. https://doi.org/10.1016/j.atmosenv.2019.02.034.

Zhu, K., Zhang, J.F., Lioy, P.J., 2007. Evaluation and comparison of continuous fine particulate matter monitors for measurement of ambient aerosols. J. Air Waste Manag. Assoc. 57 (12), 1499–1506. https://doi.org/10.3155/1047-3289.57.12.1499.